LASSI: A LOW-RANK AND ADAPTIVE SPARSE SIGNAL MODEL FOR HIGHLY ACCELERATED DYNAMIC IMAGING

Saiprasad Ravishankar, Brian E. Moore, Raj Rao Nadakuditi, and Jeffrey A. Fessler

Department of Electrical Engineering and Computer Science, Univerity of Michigan, MI, USA

ABSTRACT

Sparsity-based approaches have been popular in many applications in image processing and imaging. Recent research has shown the usefulness of sparsity or low-rank techniques for solving inverse problems such as those in dynamic imaging. In particular, the imaged temporal data sequence is modeled as a sum of low-rank and sparse components that are estimated from measurements. In this work, we instead decompose the temporal image sequence into a low-rank component and a component whose spatiotemporal patches are assumed sparse in some adaptive dictionary domain. We present a methodology to jointly estimate the underlying signal components and the spatiotemporal dictionary from highly undersampled measurements. Our numerical experiments demonstrate the promising performance of our scheme for dynamic magnetic resonance image reconstruction from undersampled k-t space data.

Index Terms— Dynamic imaging, Structured models, Sparse representations, Dictionary learning, Inverse problems.

1. INTRODUCTION

Sparsity-based techniques have been extremely popular in many applications in image processing and imaging. Compressed sensing (CS) [1, 2] is a popular technique that enables accurate recovery of signals or images from far fewer measurements than the number of unknowns or than required by Nyquist sampling conditions. CS assumes that the underlying signal is sparse in some transform domain or dictionary and that the measurement acquisition procedure is incoherent in an appropriate sense with the dictionary. CS has been shown to be very useful for magnetic resonance imaging (MRI) [3, 4]. MRI is a relatively slow modality because the data, which are samples in the Fourier space (or k-space) of the object, are acquired sequentially in time. CS-based MRI (CSMRI) involves undersampling the k-space data using random sampling techniques to accelerate data acquisition. CS

has been applied to parallel imaging (pMRI) [5, 6] and to dynamic MRI (dMRI) [4, 7].

CSMRI reconstructions with fixed, non-adaptive signal models (e.g., wavelets or total variation sparsity) typically suffer from artifacts at high undersampling factors [8]. Thus, there has been growing interest in image reconstruction methods where the dictionary is adapted to the data. For example, DLMRI [8] jointly estimates the image and a dictionary for the image patches from undersampled k-space measurements. The model here is that the (vectorized) image patches can be well approximated by a sparse linear combination of the columns of a learned (a priori unknown) dictionary D. Such adaptive dictionaries reflect image properties better than fixed models and can lead to better image reconstructions.

For dynamic data such as videos, there has been growing interest in decomposing the data into the sum of a low-rank (L) and a sparse (S) component [9, 10]. In this model, the L component may capture the background of the video, while the S component captures the sparse (dynamic) foreground. The L+S model has been recently shown to be promising for CS-based dynamic MRI [11]. The S component of the L+S decomposition could either be sparse by itself or sparse in some known dictionary or transform domain. While some works considered modeling the image sequence in dMRI as both low-rank and sparse (L & S) [12, 13], the more general L+S model may provide better quality reconstructions [11].

When employing the L+S model, the CS reconstruction problem can be formulated as follows:

$$(\text{P0}) \quad \min_{x_L, x_S} \frac{1}{2} \|E(x_L + x_S) - d\|_2^2 + \lambda_L \|R_1(x_L)\|_* + \lambda_S \|T x_S\|_1 .$$

In (P0), the underlying unknown dynamic object is $x = x_L + x_S \in \mathbb{C}^{N_x N_y N_t}$, where x_L and x_S are vectorized versions of space-time tensors corresponding to N_t temporal frames, each an image of size $N_x \times N_y$. The operator E is the sensing or encoding operator and d denotes the (undersampled) measurements. For parallel imaging with N_c receiver coils, applying the operator E involves frame-by-frame multiplication by coil sensitivities followed by the application of an undersampled Fourier encoding (i.e., the SENSE method) [14]. The operation $R_1(x_L)$ reshapes x_L into an $N_x N_y \times N_t$ matrix, and $\|\cdot\|_*$ denotes the nuclear norm that sums the singular

values of a matrix. The nuclear norm serves as a convex surrogate for matrix rank in (P0). Traditionally, the operator T in (P0) is a *known* sparsifying transform for x_S, and λ_L and λ_S are non-negative weights.

In this work, we extend the L+S model for dynamic data to a Low-rank + Adaptive Sparse SIgnal (LASSI) model. In particular, we decompose the underlying temporal image sequence into a low-rank component and a component whose spatiotemporal patches are assumed sparse in some *adaptive* dictionary domain. We propose a framework to jointly estimate the underlying signal components and the spatiotemporal dictionary from highly undersampled measurements. Our experiments demonstrate the promising performance of our data-driven model for dMRI reconstructions from undersampled k-t space data. In particular, we show that LASSI gives much improved reconstructions and richer decompositions compared to the conventional L+S model.

2. PROBLEM FORMULATION AND ALGORITHM

Here, we present our problem formulation for dynamic image reconstruction from undersampled measurements and an efficient algorithm for it.

2.1. Problem Formulation

We model the dynamic image data as $x = x_L + x_S$, where x_L is low-rank when reshaped into a (space-time) matrix, and we assume that the spatiotemporal (3D) patches in the vectorized tensor x_S are sparse in some adaptive dictionary domain. The proposed joint image sequence and dictionary estimation problem is as follows:

$$\text{(P1)} \min_{D,B,x_L,x_S} \frac{1}{2} \|E(x_L + x_S) - d\|_2^2 + \lambda_L \|R_1(x_L)\|_*$$
$$+ \lambda_S \left\{ \sum_{j=1}^M \|P_j x_S - D b_j\|_2^2 + \lambda_B^2 \|B\|_0 \right\}$$
$$\text{s.t. } \|B\|_\infty \le a, \text{ rank}(R_2(d_i)) \le r, \|d_i\|_2 = 1 \ \forall i.$$

Here, P_j is a patch extraction operator that extracts an $m_x \times m_y \times m_t$ spatiotemporal patch from x_S as a vector. Matrix $D \in \mathbb{C}^{m \times K}$ with $m = m_x m_y m_t$ is the dictionary and $b_j \in \mathbb{C}^K$ is the sparse code for the jth patch. We use $B \in \mathbb{C}^{K \times M}$ to denote the matrix that has the sparse codes b_j as its columns, $\|B\|_0$ counts the number of non-zeros in the matrix B, and $\lambda_B \ge 0$. The constraint $\|B\|_\infty \triangleq \max_j \|b_j\|_\infty \le a$, with $a > 0$ (typically very large) is used because the objective in (P1) is non-coercive with respect to B [15].

The atoms or columns of D, denoted by d_i, are constrained to have unit norm in (P1) to avoid scaling ambiguity between D and B [16]. We also model the reshaped dictionary atoms $R_2(d_i)$ as having rank (at most) $r > 0$, where $R_2(\cdot)$ is the operator that reshapes d_i into a $m_x m_y \times m_t$ space-time matrix. The rank constraint in (P1) enables local

low-rank and sparse modeling in x_S. Such structured dictionary learning may be less prone to over-fitting in applications involving limited or corrupted data.

Problem (P1) jointly learns a decomposition $x = x_L + x_S$ and a dictionary D along with the sparse coefficients B from the measurements d. Unlike Problem (P0), the fully-adaptive Problem (P1) is nonconvex.

2.2. LASSI Algorithm

We propose an efficient block coordinate descent-type algorithm for (P1), where, in one step, we update (D, B) keeping (x_L, x_S) fixed, and then we update (x_L, x_S) keeping (D, B) fixed. We then repeat these alternating steps in an iterative manner.

2.2.1. Update of D and B

Here, we optimize (P1) with respect to (D, B). Denoting by P the matrix that has the patches $P_j x_S$ as its columns, and with $C \triangleq B^H$, the optimization problem with respect to (D, B) can be rewritten as

$$\text{(P2)} \min_{D,C} \|P - DC^H\|_F^2 + \lambda_B^2 \|C\|_0$$
$$\text{s.t. } \|C\|_\infty \le a, \text{ rank}(R_2(d_i)) \le r, \|d_i\|_2 = 1 \ \forall i.$$

We employ block coordinate descent for (P2), where the columns c_i of C and atoms d_i of D are updated sequentially by cycling over all i values [15]. Specifically, for each $1 \le i \le K$, we solve (P2) first with respect to c_i and then with respect to d_i.

For the minimization with respect to c_i, we have the following subproblem, where $E_i \triangleq P - \sum_{k \ne i} d_k c_k^H$ is computed using the most recent estimates of the other atoms and coefficients:

$$\min_{c_i} \|E_i - d_i c_i^H\|_F^2 + \lambda_B^2 \|c_i\|_0 \text{ s.t. } \|c_i\|_\infty \le a, \quad (1)$$

The minimizer $\hat{c}_i$ of (1) is given by [15]

$$\hat{c}_i = \min\left(\left|H_{\lambda_B}\left(E_i^H d_i\right)\right|, a1_M\right) \odot e^{j\angle E_i^H d_i}, \quad (2)$$

where the hard-thresholding operator $H_{\lambda_B}(\cdot)$ zeros out vector entries with magnitude less than λ_B. Here, 1_M denotes a vector of ones of length M, "$\odot$" denotes element-wise multiplication, $\min(\cdot, \cdot)$ denotes element-wise minimum, and we choose a such that $a > \lambda_B$. For a vector $c \in \mathbb{C}^M$, $e^{j\angle c} \in \mathbb{C}^M$ is computed element-wise, with "$\angle$" denoting the phase.

Optimizing (P2) with respect to the atom d_i while holding all other variables fixed yields the following subproblem:

$$\min_{d_i} \|E_i - d_i c_i^H\|_F^2 \text{ s.t. } \text{rank}(R_2(d_i)) \le r, \|d_i\|_2 = 1. \quad (3)$$

Let $U_r \Sigma_r V_r^H$ denote an optimal rank-r approximation to $R_2(E_i c_i)$ that is obtained using the r leading singular vectors

and singular values of the full SVD $R_2\left(E_i c_i\right) \triangleq U\Sigma V^H$. Then a global minimizer of (3), upon reshaping, is

$$R_2(\hat{d}_i) = \begin{cases} \frac{U_r \Sigma_r V_r^H}{\|\Sigma_r\|_F}, & \text{if } c_i \neq 0 \\ v, & \text{if } c_i = 0 \end{cases} \qquad (4)$$

where v is any normalized matrix with rank at most r, of appropriate dimensions (e.g., reshaped first column of the $m \times m$ identity). The proof for (4) is not included here due to space constraints and is presented elsewhere [17].

2.2.2. Update of x_L and x_S

Minimizing (P1) with respect to x_L and x_S yields the following subproblem:

$$(\text{P3}) \quad \min_{x_L, x_S} \frac{1}{2}\|E(x_L + x_S) - d\|_2^2 + \lambda_L \|R_1(x_L)\|_*$$
$$+ \lambda_S \sum_{j=1}^{M} \|P_j x_S - D b_j\|_2^2.$$

Problem (P3) is convex but nonsmooth. The objective in (P3) can be written in the form $f(x_L, x_S) + g_1(x_L) + g_2(x_S)$, with $f(x_L, x_S) \triangleq 0.5\|E(x_L + x_S) - d\|_2^2$, $g_1(x_L) \triangleq \lambda_L \|R_1(x_L)\|_*$, and $g_2(x_S) \triangleq \lambda_S \sum_{j=1}^{M} \|P_j x_S - D b_j\|_2^2$. Similar to prior work [11], we employ a proximal gradient method for solving (P3). The iterates of the proximal gradient scheme, denoted by superscript k, take the following form:

$$x_L^k = \text{prox}_{t_k g_1}(x_L^{k-1} - t_k \nabla_{x_L} f(x_L^{k-1}, x_S^{k-1})), \qquad (5)$$

$$x_S^k = \text{prox}_{t_k g_2}(x_S^{k-1} - t_k \nabla_{x_S} f(x_L^{k-1}, x_S^{k-1})), \qquad (6)$$

where the proximity function is defined as

$$\text{prox}_{t_k g}(y) = \arg\min_z \frac{1}{2}\|y - z\|_2^2 + t_k\, g(z), \qquad (7)$$

and the gradients of f are given by

$$\nabla_{x_L} f(x_L, x_S) = \nabla_{x_S} f(x_L, x_S) = E^* E(x_L + x_S) - E^* d.$$

The update in (5) corresponds to the singular value thresholding (SVT) operation [18]. Specifically, denoting by $Q\Lambda W^H$ the SVD of $R_1(\tilde{x}_L^{k-1})$, where $\tilde{x}_L^{k-1} \triangleq x_L^{k-1} - t_k \nabla_{x_L} f(x_L^{k-1}, x_S^{k-1})$, it follows from (5) and (7) [18] that $R_1(x_L^k) = Q\hat{\Lambda} W^H$, where $\hat{\Lambda}$ is a diagonal matrix with entries

$$\hat{\Lambda}_{ii} = (\Lambda_{ii} - t_k \lambda_L)^+, \qquad (8)$$

and $(\cdot)^+ = \max(\cdot, 0)$.

Let $\tilde{x}_S^{k-1} \triangleq x_S^{k-1} - t_k \nabla_{x_S} f(x_L^{k-1}, x_S^{k-1})$. Then it follows from (6) and (7) that x_S^k satisfies the Normal equation

$$\left(I + 2t_k \lambda_S \sum_{j=1}^{M} P_j^T P_j\right) x_S^k = \tilde{x}_S^{k-1} + 2t_k \lambda_S \sum_{j=1}^{M} P_j^T D b_j. \qquad (9)$$

Solving (9) for x_S^k is straightforward because the matrix premultiplying x_S^k is diagonal, and thus its inverse can be computed cheaply.

The proximal gradient method for (P3) has been shown to converge [19] for a constant step-size $t_k = t < 2/\ell$, where ℓ is the Lipschitz constant of $\nabla f(x_L, x_S)$. For (P3), $\ell = 2\|E\|_2^2$.

3. NUMERICAL EXPERIMENTS

3.1. Framework

Here, we illustrate the performance of our method for dMRI reconstruction from k-t space data. We perform simulations with the Cartesian cardiac perfusion data used in prior work [11]. The data were acquired with a modified TurboFLASH sequence on a 3T scanner using a 12-element coil array. Fully-sampled perfusion image data with an image matrix size of 128×128 and 40 temporal frames was acquired with FOV $= 320 \times 320$ mm^2, slice thickness $= 8$ mm, spatial resolution $= 3.2$ mm^2, and temporal resolution of 307 ms.

The fully-sampled data were retrospectively undersampled using a different variable-density random Cartesian undersampling pattern along k_y for each time frame. We simulate several undersampling (acceleration) factors, each with a new randomly generated undersampling pattern, in our experiments. We measure the quality of the dMRI reconstructions using the normalized root mean square error (NRMSE) metric defined as

$$\text{NRMSE} = \frac{\|x_{\text{recon}} - x_{\text{ref}}\|_2}{\|x_{\text{ref}}\|_2}, \qquad (10)$$

where x_{ref} is a reference reconstruction from the fully-sampled data, and x_{recon} is the reconstruction from undersampled data.

We compare the quality of reconstructions obtained with the proposed LASSI method to those obtained with the recent L+S method [11]. For the L+S method, we used the publicly available MATLAB implementation [20] with T set to a temporal Fourier transform, and we chose the parameters λ_L and λ_S by sweeping over a range of values and choosing the settings that achieved the best NRMSE in our experiments. Specifically, we set $\lambda_L = 0.525$ and $\lambda_S = 0.01$, and we ran the L+S method for 250 iterations to ensure convergence.

For the LASSI method, we set $\lambda_L = 0.5$, $\lambda_S = 0.01$, and $\lambda_B = 0.03$. We extracted spatiotemporal patches of size $8 \times 8 \times 5$ from x_S in (P1) with spatial and temporal patch overlap strides of 2 pixels, and we set $r = 1$. We ran LASSI for 50 outer iterations with 1 and 5 inner iterations in the (D, B) and (x_L, x_S) updates, respectively. Since Problem (P1) is nonconvex, the proposed algorithm needs to be initialized appropriately. We initialized D with the 320×320 DCT, initialized $B = 0$, and initialized x_L and x_S with the output of the L+S method with $\lambda_L = 1.2$ and $\lambda_S = 0.01$.
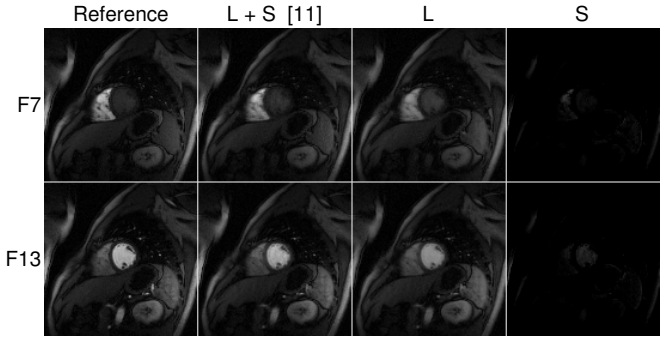
Fig. 1. 8x undersampling: Frames 7 and 13 of the conventional L+S reconstruction [11] along with the corresponding reference frames. The low-rank (L) and sparse (S) components of each reconstructed frame are also individually shown. Only image magnitudes are displayed.
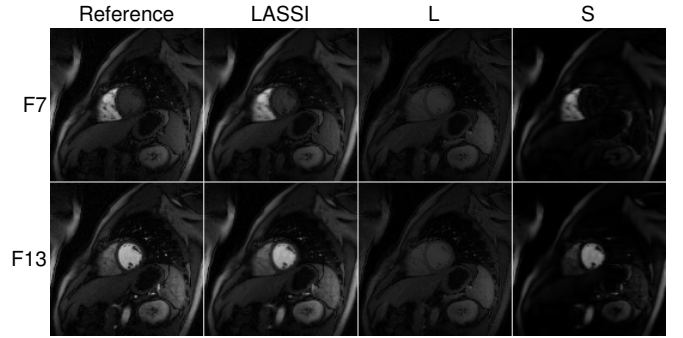
Fig. 2. 8x undersampling: Frames 7 and 13 of the proposed LASSI reconstruction along with the corresponding reference frames. The low-rank (L) and adaptive dictionary-sparse (S) components of each reconstructed frame are also individually shown. Only image magnitudes are displayed.

Undersampling	20x	16x	12x	8x	4x
NRMSE (L+S) %	21.0	17.8	15.6	13.7	10.9
NRMSE (LASSI) %	**20.6**	**17.0**	**14.5**	**12.5**	**10.2**
Improvement (dB)	0.17	0.40	0.64	0.80	0.58

Table 1. NRMSE values expressed as percentages for the L+S [11] and LASSI methods at several undersampling (acceleration) factors. The best NRMSE values for each undersampling rate are marked in bold, and the improvement by LASSI in each case is indicated in decibels (dB).

Fig. 3. Zoomed-in views of Frame 13 of the reconstructions in Figures 1 and 2. The arrows highlight that the proposed LASSI reconstruction more accurately recovers the contrast seen in the reference reconstruction than the conventional L + S reconstruction [11].

3.2. Results

Table 1 lists the NRMSE values as percentages for the L+S [11] and LASSI methods at various undersampling factors of k-t space. The proposed LASSI method provides lower reconstruction error for each undersampling factor tested. In particular, the adaptive sparse modeling of the x_s component of LASSI yields NRMSE improvements up to 0.8 dB. In our experiments, we observed small NRMSE improvements using the $r = 1$ constraint on the reshaped dictionary atoms (used in Table 1) compared to the full-rank ($r = 5$) case [17].

Figures 1 and 2 show reconstructions of two representative frames produced by the L+S and LASSI methods, respectively, with eightfold undersampling of k-t space. The LASSI reconstructions are sharper and a better approximation of the reference frames (i.e., fully-sampled reconstructions) shown. Figs. 1 and 2 also show the x_L and x_S components of the reconstructed frames. In particular, the x_L component of the LASSI reconstruction is clearly low-rank, and the x_S component captures the changes in contrast and other dynamic features in the data. On the other hand, the x_L component of the conventional L+S reconstruction varies more over time (i.e., it has higher rank), and the x_S component contains relatively little information. The richer (x_L, x_S) decomposition produced

by LASSI suggests that both the low-rank and adaptive-sparse components of the model are well-suited for dMRI.

Figure 3 shows zoomed-in views of the reconstructions from Figs. 1 and 2. The proposed LASSI method produces images with better contrast along the myocardial wall compared to the conventional L+S method, and more accurately reflects the reference reconstruction.

4. CONCLUSIONS

In this work, we investigated a novel framework for reconstructing spatiotemporal data from highly undersampled measurements. The proposed framework jointly learns a low-rank and dictionary-sparse decomposition of the underlying image sequence together with a spatiotemporal dictionary. The proposed algorithm involves simple and efficient updates. Our experimental results show the potential of our method for accelerated dynamic MR imaging compared to recent works. We present more extensive results elsewhere [17]. The usefulness of our scheme in other inverse problems and image processing applications merits further study.

5. REFERENCES

[1] D. Donoho, "Compressed sensing," *IEEE Trans. Information Theory*, vol. 52, no. 4, pp. 1289–1306, 2006.

[2] E. Candès, J. Romberg, and T. Tao, "Robust uncertainty principles: exact signal reconstruction from highly incomplete frequency information," *IEEE Trans. Information Theory*, vol. 52, no. 2, pp. 489–509, 2006.

[3] M. Lustig, D.L. Donoho, and J.M. Pauly, "Sparse MRI: The application of compressed sensing for rapid MR imaging," *Magnetic Resonance in Medicine*, vol. 58, no. 6, pp. 1182–1195, 2007.

[4] M. Lustig, J. M. Santos, D. L. Donoho, and J. M. Pauly, "k-t SPARSE: High frame rate dynamic MRI exploiting spatio-temporal sparsity," in *Proc. ISMRM*, 2006, p. 2420.

[5] D. Liang, B. Liu, J. Wang, and L. Ying, "Accelerating SENSE using compressed sensing," *Magnetic Resonance in Medicine*, vol. 62, no. 6, pp. 1574–1584, 2009.

[6] R. Otazo, D. Kim, L. Axel, and D. K. Sodickson, "Combination of compressed sensing and parallel imaging for highly accelerated first-pass cardiac perfusion MRI," *Magnetic Resonance in Medicine*, vol. 64, no. 3, pp. 767–776, 2010.

[7] U. Gamper, P. Boesiger, and S. Kozerke, "Compressed sensing in dynamic MRI," *Magnetic Resonance in Medicine*, vol. 59, no. 2, pp. 365–373, 2008.

[8] S. Ravishankar and Y. Bresler, "MR image reconstruction from highly undersampled k-space data by dictionary learning," *IEEE Trans. Med. Imag.*, vol. 30, no. 5, pp. 1028–1041, 2011.

[9] E. J. Candès, X. Li, Y. Ma, and J. Wright, "Robust principal component analysis?," *J. ACM*, vol. 58, no. 3, pp. 11:1–11:37, 2011.

[10] H. Guo, C. Qiu, and N. Vaswani, "An online algorithm for separating sparse and low-dimensional signal sequences from their sum," *IEEE Transactions on Signal Processing*, vol. 62, no. 16, pp. 4284–4297, 2014.

[11] R. Otazo, E. Candès, and D. K. Sodickson, "Low-rank plus sparse matrix decomposition for accelerated dynamic MRI with separation of background and dynamic components," *Magnetic Resonance in Medicine*, vol. 73, no. 3, pp. 1125–1136, 2015.

[12] S. G. Lingala, Y. Hu, E. DiBella, and M. Jacob, "Accelerated dynamic MRI exploiting sparsity and low-rank structure: k-t SLR," *IEEE Transactions on Medical Imaging*, vol. 30, no. 5, pp. 1042–1054, 2011.

[13] B. Zhao, J. P. Haldar, A. G. Christodoulou, and Z. P. Liang, "Image reconstruction from highly undersampled (**k**, t) -space data with joint partial separability and sparsity constraints," *IEEE Transactions on Medical Imaging*, vol. 31, no. 9, pp. 1809–1820, 2012.

[14] K. P. Pruessmann, M. Weiger, P. Börnert, and P. Boesiger, "Advances in sensitivity encoding with arbitrary k-space trajectories," *Magnetic Resonance in Medicine*, vol. 46, no. 4, pp. 638–651, 2001.

[15] S. Ravishankar, R. R. Nadakuditi, and J. A. Fessler, "Efficient sum of outer products dictionary learning (SOUP-DIL) - the ℓ_0 method," 2015, Preprint: `http://arxiv.org/abs/1511.08842`.

[16] R. Gribonval and K. Schnass, "Dictionary identification–sparse matrix-factorization via l_1 - minimization," *IEEE Trans. Inform. Theory*, vol. 56, no. 7, pp. 3523–3539, 2010.

[17] S. Ravishankar, B. E. Moore, R. R. Nadakuditi, and J. A. Fessler, "Low-rank and adaptive sparse signal (LASSI) models for highly accelerated dynamic imaging," 2016, to be submitted.

[18] J-F Cai, E. J. Candès, and Z. Shen, "A singular value thresholding algorithm for matrix completion," *SIAM Journal on Optimization*, vol. 20, no. 4, pp. 1956–1982, 2010.

[19] P. L. Combettes and V. R. Wajs, "Signal recovery by proximal forward-backward splitting," *Multiscale Modeling & Simulation*, vol. 4, no. 4, pp. 1168–1200, 2005.

[20] R. Otazo, "L+S reconstruction matlab code," `http://cai2r.net/resources/software/ls-reconstruction-matlab-code`, 2014, [Online; accessed Mar. 2016].